Traveling-Wave Inverted-Gate Field-Effect Transistors: Concept, Analysis, and Potential

SAMIR M. EL-GHAZALY, MEMBER, IEEE, AND TATSUO ITOH, FELLOW, IEEE

Abstract—**The inverted-gate FET (INGFET) is very promising as a traveling-wave transistor. A unified approach to the analysis of the traveling-wave INGFET is presented. The equivalent circuit parameters of the GaAs inverted-gate FET, with submicron gate length, are obtained using a two-dimensional computer model which takes into account the nonstationary electron dynamics. The parameters of the passive transmission line, corresponding to the INGFET structure, are obtained using a quasi-TEM wave approach. The conductor losses of this structure are estimated using the incremental inductance rule. The coupled mode theory is used to derive the wave equation describing this traveling-wave transistor. The results show the existence of a rapidly growing mode along the device electrodes. It is also shown that this mode can be excited alone by appropriate matching and feeding arrangements. Improper matching and feeding lead to a narrower bandwidth due to the resonance phenomenon of the resulting standing wave.**

I. INTRODUCTION

TRAVELING-WAVE transistors are believed to provide high gain and high power amplification over a very wide frequency band. On the other hand, the limitation on the transistor width is removed when it is operated in the traveling-wave mode. In the conventional transistors, this width is limited by two factors, namely, the signal attenuation along the input electrode and the phase velocity mismatch between the signals on the input and output electrodes. The second factor can be understood by knowing that in the millimeter-wave range the transistor electrodes act as transmission lines since the device width becomes comparable to the wavelength. The input transmission line, the gate electrode, has a different reactance from the output transmission line, the drain electrode. Therefore, they exhibit different phase velocities for the input and output signals. The transistor width is limited to 0.1 wavelength to avoid the phase cancellation due to the phase velocity mismatch. El-Ghazaly and Itoh [1], [2] analyzed the dc characteristics of inverted-gate FET (INGFET) structures and showed that these transistors are very promising for traveling-wave transistor operation. The main advantages of these transistors are as follows:

1) The phase velocity on the input line, the source electrode, and the output line, the drain electrode, are matched in the quiescent case, owing to the device symmetry around its ground line (i.e., gate electrode). Once the dc bias is applied, the phase velocities become slightly mismatched. However, they remain close to each other. This allows the realization of wide transistors and results in a more efficient traveling-wave operation.
2) The gate electrode is realized with a very large cross-sectional area compared to conventional MESFET structures. This practically eliminates the parasitic gate resistance, which is the main source of the input signal attenuation and a major contributor to the device noise.
3) Owing to the high transconductance of the intrinsic INGFET [2] and also to the phase velocity match, this device is capable of producing a high wave growth factor along its electrodes, which means high gain from a single transistor unit.
4) This device has a very small thermal resistance since its metallic gate electrode is very close to the hot region inside the active layer. The gate electrode can be directly connected to the heat sink. However, if one desires to electrically isolate the gate from the heat sink (i.e, the lower ground plane) for dc bias purposes, a thin layer of dielectric material can be introduced, as shown in Fig. 1. Such a thin layer does not affect the thermal conductivity very much.

The traveling-wave transistor has been studied using theoretical and experimental approaches [3]–[10]. These studies were performed using conventional MESFET structures. Many of the theoretical approaches are based on the small-signal equivalent circuit of the transistor which can be measured or calculated. This equivalent circuit is combined with the transmission line system to obtain the wave propagation characteristics along the transistor width. In this paper, we will present a complete approach for analyzing the traveling-wave transistor including the evaluation of the small-signal transistor model,

Manuscript received August 9, 1988; revised December 29, 1988. This work was supported by the U.S. Army Research Office under Contract DAAL03-88-k-0005.

S. M. El-Ghazaly was with the Department of Electrical and Computer Engineering, University of Texas at Austin, Austin, TX. He is now with the Department of Electrical and Computer Engineering, Arizona State University, Tempe, AZ 85287.

T. Itoh is with the Department of Electrical and Computer Engineering, University of Texas at Austin, Austin, TX 78712.

IEEE Log Number 8927162.

0018-9480/89/0600-1027$01.00 ©1989 IEEE

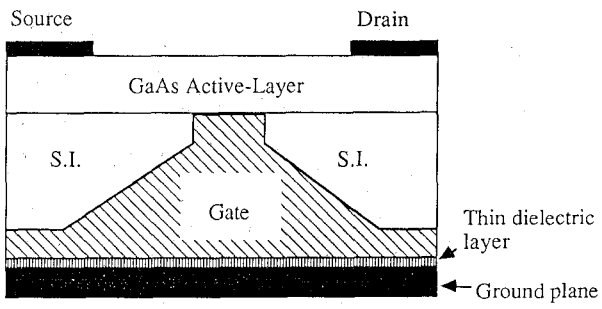

Fig. 1. The INGFET structure.

the transmission line model, and the system losses. The effect of the electrode terminations is thoroughly investigated to analyze its effect on the device gain. This approach allows the user to theoretically optimize the FET structure, the electrode dimensions, and the terminations of the input and the output device lines before starting the fabrication process. This approach is applied to investigate the potential of the traveling-wave INGFET. However, it can be applied to any traveling-wave transistor.

II. The Analysis

The full analysis can be summarized in four basic steps. First, the active transistor (INGFET) characteristics are accurately calculated. Second, the parameters of the cylindrical transmission line, with arbitrary shape in the cross section, are evaluated. Third, the coupled mode theory is used to formulate the wave equation along the transmission line using the results of the first two steps. Fourth, the resulting eigenvalue problem is solved to obtain the propagation constants, the characteristics modes (i.e., the eigenvectors), and the characteristic impedances. Hence, one can solve the excitation problem to obtain the gain and the optimal device terminations.

Step 1: The INGFET Characterization

This step is carried out by using a two-dimensional computer model which simultaneously solves the continuity equation, the energy conservation equation, and Poisson's equation. The electron mobility and temperature are functions of the average electron energy. This model is capable of accurately simulating the submicron-gate GaAs MESFET's since such nonstationary conditions as velocity overshoot are taken into consideration. This model was applied to investigate the INGFET characteristics [1], [2]. It is shown that for a gate length of 0.5 μm, the INGFET produces a transconductance as high as 300 mS/mm and a current-gain cutoff frequency that exceeds 65 GHz. Shorter gates result in higher transconductances and higher cutoff frequencies. The small-signal equivalent circuit of the INGFET employed here is based on the results published in [2].

Step 2: The Transmission Line Characterization

The passive transmission line cross section is shown in Fig. 2. Considering that the source-to-drain separation is very short, about 1.5 μm, and that the active-layer thickness is 0.1 ~ 0.2 μm, it can easily be seen that the quasi-TEM solution is quite acceptable in the lower millimeter-wave range. Hence, the transmission line parameters (i.e., the capacitances and the inductances) can be obtained by solving the appropriate form of Laplace equation in the cross section:

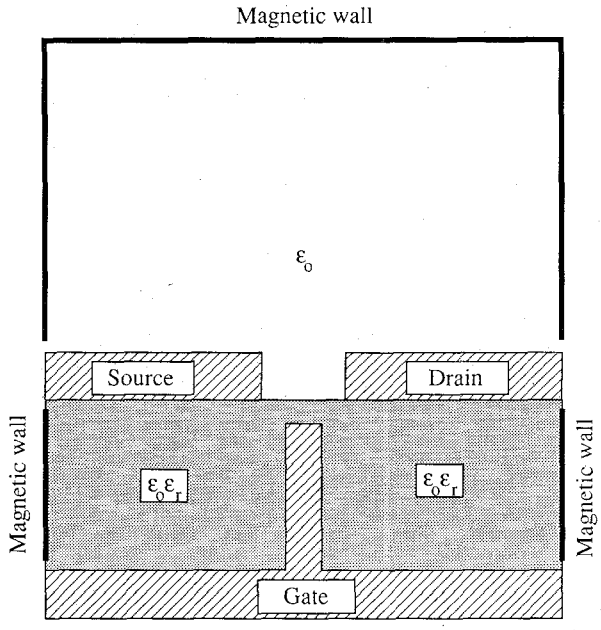

Fig. 2. The transmission line model of the INGFET (not to scale).

$$\nabla \cdot (\epsilon \nabla V) = 0. \tag{1}$$

This equation is reduced to the normal form of the Laplace equation away from the air–dielectric interface. Magnetic walls are used in the top boundary as well as on the sides. These magnetic walls can be justified in two ways. For the structure shown in Fig. 2, the gap between the electrodes is very narrow compared to the other dimensions. Therefore, most of the energy is concentrated in the gap between the conductors. The field becomes practically negligible as we move away from the center. On the other hand, several transistor units are placed in parallel in the practical realization. Hence, the symmetry of the resulting structure justifies the magnetic wall.

Because of its simplicity, the finite difference scheme is used to solve the Laplace equation. Once the potential distribution is computed, the charge distribution and the capacitances are easily derived. By performing the solution for the even and odd excitations separately, the self- and mutual capacitances are identified.

To solve for the inductances, it is assumed that the solution for the magnetic field is not affected by the presence of the dielectric. This assumption is acceptable for quasi-TEM solutions. Therefore, the Laplace equation is solved again with $\epsilon_r = 1$ to obtain the capacitance of the transmission line in free space. Knowing that the phase velocity of a TEM wave in free space is independent of the transmission line geometry, the inductance can be deduced

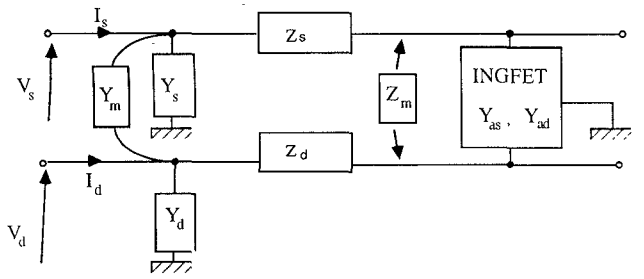

Fig. 3. The coupled-active transmission line circuit.

from the capacitance using the relation

$$v = \frac{1}{\sqrt{LC}} \tag{2}$$

where v is the velocity of light in free space and L and C are the inductance and the capacitance of the transmission line per unit length. Again, by repeating the solution for the even and odd excitations, the self- and mutual inductances can be identified.

To estimate the conductor loss, the incremental inductance rule is used [11]. Briefly, this rule relates the conductor losses (which define the resistance R) to the difference between the inductance of the original structure and that of another structure in which all the surfaces are recessed by half the skin depth. The channel loss is accounted for by using source and drain resistances, R_s and R_d, respectively. R_s is estimated by considering the source–gate region as ohmic resistance [12]:

$$R_s = \frac{L_{gs}}{qn_0\mu a} \tag{3}$$

where L_{gs} is the gate–source separation, q is the electron charge, n_0 is the electron concentration, μ is the mobility, and a is the active-layer thickness. R_d is obtained from the transistor I–V characteristics in the saturation region.

Step 3: Formulation of the Coupled Mode Equations

Once the equivalent circuit of the INGFET and the transmission line parameters are obtained, one can formulate the equations relating the voltages and currents on this coupled active line [3]–[5]. Based on Fig. 3, the equations can be in the form

$$\frac{\partial V_s}{\partial z} + I_s Z_s + I_d Z_m = 0 \tag{4a}$$

$$\frac{\partial I_s}{\partial z} + V_s(Y_s + Y_{as}) + V_d Y_m' = 0 \tag{4b}$$

$$\frac{\partial V_d}{\partial z} + I_d Z_d + I_s Z_m = 0 \tag{4c}$$

$$\frac{\partial I_d}{\partial z} + V_d Y_d + V_s(Y_m' + Y_{ad}) = 0. \tag{4d}$$

Here V_s and V_d are the source and drain voltages, respectively, and I_s and I_d are the source and drain currents, respectively. The other elements are as shown in Fig. 3. The exact expressions for the circuit parameters (Z_s, Z_d, Y_s, Y_d, Y_m', etc.) are obtained using simple circuit concepts. It should be noted that some parts of the INGFET small-signal equivalent circuit are included in Z_s, $Z_d Y_m'$. The variables are differentiated with respect to the z axis, along the device width. The voltages and the currents are replaced by the equivalent expressions of the incident and reflected waves on the line. Finally the equations become

$$\frac{\partial}{\partial z}\boldsymbol{x} + A\boldsymbol{x} = 0 \tag{5}$$

where $\boldsymbol{x}^T[S^+S^-D^+D^-]$ is a vector containing the coefficients of the incident wave on the source line, S^+, the reflected wave on the source line, S^-, the incident wave on the drain line, D^+, and the reflected wave on the drain line, D^-. A is a 4×4 complex matrix containing the network parameters per unit length.

Step 4: The Solution

The matrix equation (5) is solved for the eigenvalues and the eigenvectors which represent the possible propagation constants (γ) and the corresponding modes respectively. Knowing the modal solution, one can consider the case of an active transmission line of length W, which corresponds to a transistor of width W, with the proper terminations and excitations. Hence, the total gain from the transistor unit and the optimal input and output impedances on the source and drain lines can be evaluated.

III. Results

The previously described approach was applied to study an INGFET structure which consists of a GaAs active layer of 0.1 μm thickness. The source-to-drain separation is 1.5 μm. The gate length is 0.5 μm. All the metallic electrodes are considered to be made of copper. The source and drain electrodes are 10 μm long.

The propagation constants of the source and drain modes, at a dc bias condition suitable for power operation, of the INGFET are shown in Fig. 4. Propagation of the type $e^{-(\alpha+j\beta)z}$ is assumed. It is shown that two different modes may exist in this device. One mode has a negative α, which means that its amplitude is growing as it propagates along the device width. For the other mode, α is positive, which indicates that this mode is lossy. It is also observed that the growing mode is slightly slower than the lossy mode. By comparing these results with the other published data, [5] and [7], one observes that this device has a larger growth factor, α_{gain}, and a smaller loss factor, α_{loss}, than the conventional MESFET operated as a traveling-wave transistor. This is due to the reduced conductor losses in the gate electrode and the positive feedback in the case of the INGFET. To explain the latter reason, one should notice that the feedback capacitance, in this configuration, is C_{ds}. Simple transistor circuit theory shows that this leads to a positive feedback amplifier. Two curves are provided for the α_{gain}. One curve (—o—o—) is obtained with both the conductor losses and the channel losses taken into consideration. The other curve (– – –) is obtained by considering the conductor losses only. This curve

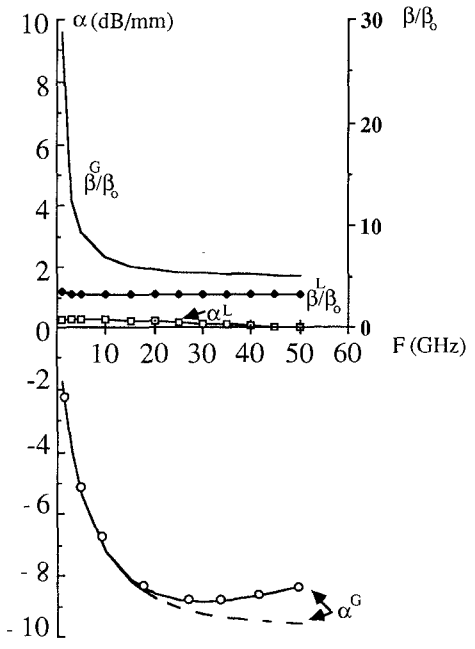

Fig. 4. The propagation constants of the possible modes on the traveling-wave INGFET. Superscript G denotes the gainful mode and superscript L denotes the lossy mode. For α^G, the line (—o—o—) is obtained considering both conductor and channel losses; the other curve (---) is obtained considering conductor losses only.

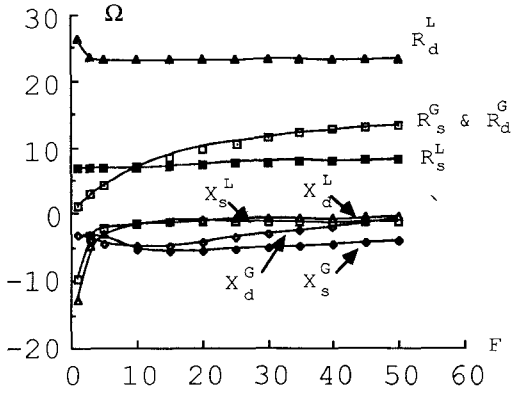

Fig. 5. The modal characteristic impedances. Superscript G denotes the gainful mode and superscript L denotes the lossy mode.

allows the reader to extract and analyze the characteristics of the pure traveling-wave transistor without indulging in the controversy associated with estimating the channel losses. It should be noted that the goal of this research is to demonstrate the potential of the traveling-wave INGFET rather than to give design data, at least in this stage. Therefore, the latter curve is used in the following study.

The modal characteristic impedances, defined as the voltage to current ratio for each line with respect to ground, are shown in Fig. 5. The growing mode has about the same resistive parts on the source and drain lines. However, the reactive parts are slightly different. The resistive part of the lossy mode on the drain line is significantly higher. One should notice that in order to excite the growing mode only, the device must be terminated in the characteristic impedance of this mode, and the input signal

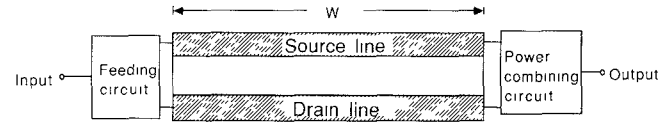

Fig. 6. The circuit arrangements required to excite the pure TWT mode.

has to be fed to both lines simultaneously with the appropriate relative amplitudes and phases. These relative amplitudes and phases are obtained from the eigenvectors of (5). This mode represents the genuine traveling-wave transistor operation, and we will refer to it as the pure TWT mode. The calculations show that a substantial amount of power exists at the output port of the source line as well as the drain line. Bearing in mind that the characteristic impedances of the source and drain lines are very close, it is suggested that a simple power combining circuit be added to the output as shown in Fig. 6. This may increase the gain by up to 3 dB.

The device gain is defined as

$$G = 10 \log \left[\frac{\text{power output}}{\text{power available at the input}} \right]. \quad (6)$$

This gain will be investigated using several device terminations:

1) Pure TWT mode, in which only the growing mode is excited. If one does not consider a power combining circuit in the output, a maximum of 3 dB has to be subtracted from the given gain.
2) Maximum output power conditions, which is the same as the pure TWT mode except that the output impedances are the complex conjugate of the characteristic impedance of the lines. It will be called maximum power load in the following text.
3) Pure resistive load (10 Ω) at all the ports. The signal is directly fed to the input ports without adjusting either the relative amplitudes or the phases. No power combining circuit is used at the output.
4) Selected practical load, which is close to the characteristic impedance at 25 GHz at the input ports and its complex conjugate at the output ports. It will be called practical load. No power combining circuit is used.

The gain variation with these four loads as a function of the device width is shown in Fig. 7 at 25 GHz. It is shown that the pure TWT mode results in a gain that increases linearly with the device width, as expected. Of course, this result is acceptable as long as the small-signal analysis is valid. The maximum power load produces a gain that is very close to the traveling-wave transistor mode for narrow device. Its gain fluctuates for the wide device, 4 ~ 5 mm, due to the increasing effect of the reflected wave. The 10 Ω resistive load is acceptable for a relatively narrow device, less than 2 mm. The performance is degraded very rapidly as the device gets wider. The selected practical load represents a reasonable compromise between the other terminations.

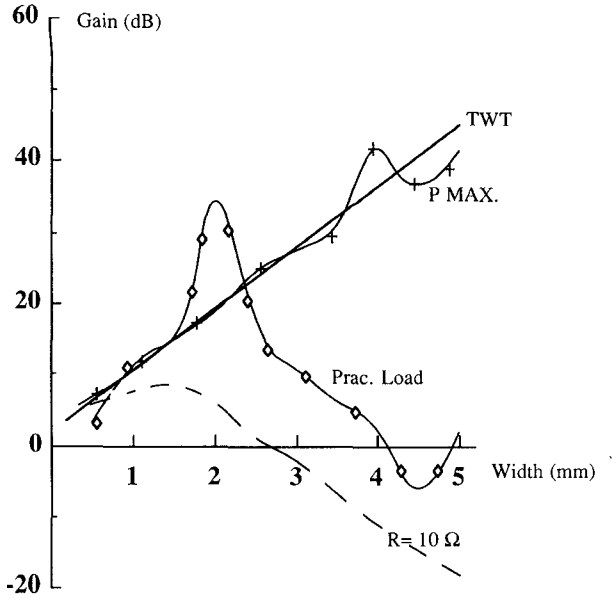

Fig. 7. The gain as function of the transistor width at 25 GHz. —— TWT mode; —+—+— maximum power mode; --- 10 Ω resistive load; —◇—◇— practical load.

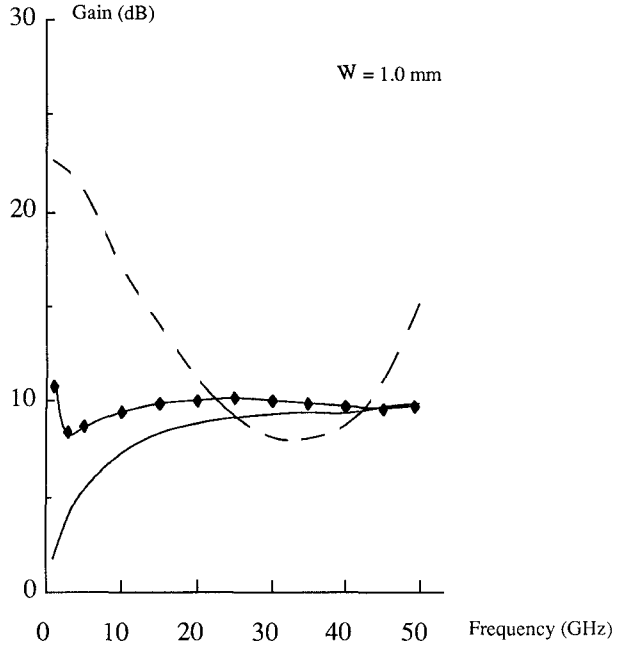

Fig. 8. The gain versus frequency for different modes. —— the pure TWT mode; —◆—◆— maximum power mode; --- 10 Ω resistive load.

Fig. 8 shows the gain performance with the frequency for devices of 1 mm width. The traveling-wave transistor mode and the maximum power load produce a flat gain over a very wide band frequency. This clearly manifests the advantage of the traveling-wave transistor. The 10 Ω case starts by a high gain at low frequency, and then the gain drops. This may be explained by knowing that a 1 mm device, below 10 GHz, behaves like a lumped transistor, and the traveling-wave operation is not significant at such a relatively low frequency. The selected impedance case is shown in Fig. 9. Three different device

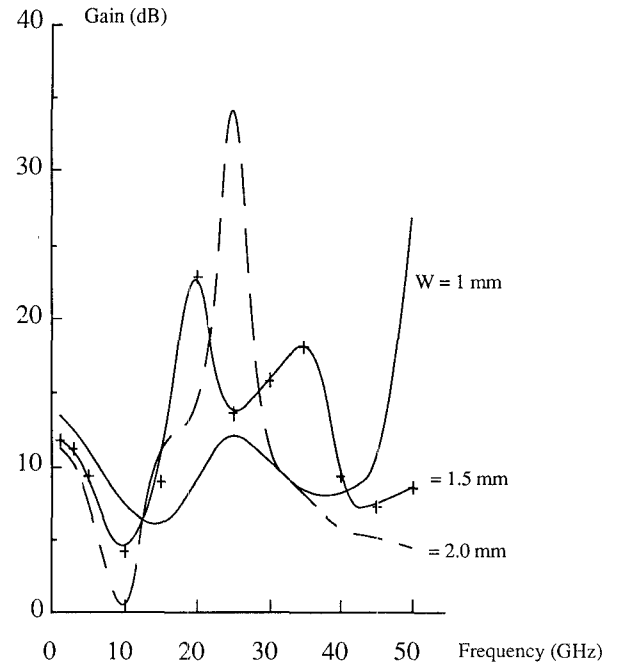

Fig. 9. The gain as function of frequency for the selected "practical impedance termination" at different device widths.

widths are considered. It is observed that the gain of the narrow device, $W=1$ mm, has a smaller ripple in the midband. The wider devices produce more gain but with more gain fluctuations due to the resonance phenomenon.

In the practical realization of the INGFET–TWT, the stability conditions of this device have to be carefully considered since it is a very high gain device. In addition to the other stability factors considered in any amplifier, the drain-to-source capacitance (C_{ds}) should be carefully designed due to its role as a positive feedback element. Moreover, the device terminations and the device length must be selected to result in a reflected wave which is smaller than the incident wave at the input port. The latter condition is required to ensure that the input power is always positive (i.e., positive input resistance).

IV. Conclusion

A unified approach for analyzing the complicated traveling-wave transistor is presented. It starts by solving the two-dimensional semiconductor equations to obtain the transistor model which represents the active part of the problem. The passive transmission line parameters are evaluated separately. The wave equation is formulated using the coupled mode theory to solve for the possible modes on this active transmission line.

The INGFET has many interesting electronic, electromagnetic, and thermal features which make it a powerful candidate for traveling-wave transistor operation. The results show that the INGFET exhibits a fast growing mode along its electrodes. To operate in the traveling-wave transistor mode, the input and output impedances of the four ports must be matched, and the signal has to be fed to the source and drain lines simultaneously with the appropriate

amplitudes and relative phases. This mode guarantees a flat frequency response over a very wide frequency band. Moreover, the gain is linearly increased with the device width. However, such a configuration is hard to realize due to the difficulties in matching the impedances and designing the feeding network. Several practical loads may be used to obtain a high gain, a wide bandwidth, or both. These loads can be selected using an appropriate optimization process.

References

[1] S. El-Ghazaly and T. Itoh, "Inverted-gate GaAs MESFET characteristics," in *Proc. 17th European Microwave Conf.* (Rome), 1987, pp. 113–118.

[2] S. El-Ghazaly and T. Itoh, "Inverted-gate GaAs field-effect transistors: Novel high-frequency structures," *IEEE Trans. Electron Devices*, vol. ED-35, pp. 810–817, 1988.

[3] A. Holden, D. Daniel, I. Davies, C. Oxley, and H. Rees, "Gallium arsenide traveling-wave field-effect transistors," *IEEE Trans. Electron Devices*, vol. ED-32, pp. 61–66, 1985.

[4] W. Heinrich, "Distributed equivalent-circuit model for traveling-wave FET design," *IEEE Trans. Microwave Theory Tech.*, vol. MTT-35, pp. 487–491, May 1987.

[5] K.-H. Kretschmer, P. Grambow, and T. Sigulla, "Coupled-mode analysis of traveling-wave MESFETs," *Int. J. Electron.*, vol. 58, pp. 639–648, 1985.

[6] A. Podgorski and L. Wei, "Theory of traveling-wave transistors," *IEEE Trans. Electron Devices*, vol. ED-29, pp. 1845–1853, Dec. 1982.

[7] K. Fricke and H. Hartnagel, "GaAS MESFET optimization and new device applications based on wave property studies," in *IEEE-MTT's Dig.*, 1985, pp. 192–195.

[8] K. Fricke and H. Hartnagel, "Experimental study of MESFET traveling-wave structures," *Int. J. Electron.*, vol. 58, pp. 629–638, 1985.

[9] Y. Ayasli, L. Reynolds, R. Mozzi, and L. Hanes, "2–20-GHz traveling-wave power amplifier," *IEEE Trans. Microwave Theory Tech.*, vol. MTT-32, pp. 290–294, Mar. 1984.

[10] Y.-A. Ren, G.-H. Ruan, and H. Hartnagel, "Microwave structuring of MESFET electrodes for increased power and efficiency," in *Proc. IEEE-IEDM*, 1981, pp. 684–687.

[11] H. Wheeler, "Transmission-line properties of a strip on a dielectric sheet on a plane," *IEEE Trans. Microwave Theory Tech.*, vol. MTT-25, pp. 631–641, 1977.

[12] M. Shur and L. Eastman, "Current–voltage characteristics, small-signal parameters, and switching times of GaAs FET's," *IEEE Trans. Electron Devices*, vol. ED-25, pp. 606–611, June 1978.

✠

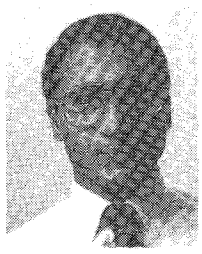

Samir M. El-Ghazaly was born in Luxor, Egypt, on July 1, 1959. He received the B.Sc. degree in electronics and communications engineering (Distinction, Honors) in 1981 and the M.Sc. degree in 1984, both from Cairo University, Cairo, Egypt, and the Ph.D. degree, in electrical engineering, from the University of Texas at Austin in 1988.

He was appointed as a Teaching Assistant in the Department of Electronics and Communication Engineering, Cairo University, in October 1981, and became Assistant Lecturer in 1984. From November 1982 to October 1983, he was with the Centre Hyperfrequences et Semiconducteurs, Université de Lille I, Lille, France, where he worked on the simulation of submicronic-gate MESFET's. In January 1984 he joined the Department of Electrical Engineering, University of Ottawa, Canada, where he worked on the analysis of *E*-plane circuits. In September 1986 he joined the Department of Electrical and Computer Engineering at the University of Texas at Austin as a research assistant and became a Post-Doctoral Fellow in 1988. In September 1988, he joined Arizona State University, Tempe, AZ, as an Assistant Professor.

✠

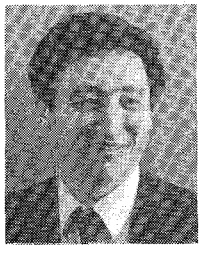

Tatsuo Itoh (S'69–M'69–SM'74–F'82) received the Ph.D. degree in electrical engineering from the University of Illinois, Urbana, in 1969.

From September 1966 to April 1976, he was with the Electrical Engineering Department, University of Illinois. From April 1976 to August 1977, he was a Senior Research Engineer in the Radio Physics Laboratory, SRI International, Menlo Park, CA. From August 1977 to June 1978, he was an Associate Professor at the University of Kentucky, Lexington. In July 1978, he joined the faculty at the University of Texas at Austin, where he is now a Professor of Electrical Engineering and Director of the Electrical Engineering Research Laboratory. During the summer of 1979, he was a guest researcher at AEG-Telefunken, Ulm, West Germany. Since September 1983, he has held the Hayden Head Centennial Professorship of Engineering at the University of Texas. In September 1984, he was appointed Associate Chairman for Research and Planning of the Electrical and Computer Engineering Department. He also holds an Honorary Visiting Professorship at the Nanjing Institute of Technology, China.

Dr. Itoh is a member of Sigma Xi and of the Institute of Electronics and Communication Engineers of Japan. He is a member of Commission B and Chairman of Commission D of USNC/URSI. He served as the Editor of the IEEE TRANSACTIONS ON MICROWAVE THEORY AND TECHNIQUES for 1983–1985. He serves on the Administrative Committee of the IEEE Microwave Theory and Techniques Society. Dr. Itoh is a Professional Engineer registered in the state of Texas.